

iLocScan: Harnessing Multipath for Simultaneous Indoor Source Localization and Space Scanning

Chi Zhang Feng Li Jun Luo Ying He

School of Computer Engineering
Nanyang Technological University

{czhang8, fli3, junluo, yhe}@ntu.edu.sg

Abstract

Whereas a few physical layer techniques have been proposed to locate a signal source indoors, they all deem multipath a “curse” and hence take great efforts to cope with it. Consequently, each sensor only obtains the information about the direct path; this necessitates a networked sensing system (hence higher system complexity and deployment cost) with at least three sensors to actually locate a source.

In this paper, we deem multipath a “bless” and thus innovatively exploit the power of it. Essentially, with minor knowledge of the geometry of an indoor space, each signal path may potentially contribute a new piece of information to the location of its source. As a result, it is possible to locate the source with only one hand-held device. At the same time, the extra information provided by multipath can help to at least partially reconstruct the geometry of the indoor space, which enables a floor plan generation process missing in most of the indoor localization systems.

To demonstrate these ideas, we implement a USRP-based radio sensor prototype named iLocScan; it can simultaneously scan an indoor space (hence generate a plan for it) and position the signal source in it. Through iLocScan, we mainly aim to showcase the feasibility of harnessing multipath in assisting indoor localization, rather than to rival existing proposals in terms of localization accuracy. Nevertheless, our experiments show that iLocScan offers satisfactory results on both source localization and space scanning.

Categories and Subject Descriptors

C.2.1 [Network Architecture and Design]: Wireless communication

General Terms

Design, Experimentations, Performance

Keywords

Indoor Source Localization, Floor Plan Generation

Permission to make digital or hard copies of all or part of this work for personal or classroom use is granted without fee provided that copies are not made or distributed for profit or commercial advantage and that copies bear this notice and the full citation on the first page. Copyrights for components of this work owned by others than ACM must be honored. Abstracting with credit is permitted. To copy otherwise, or republish, to post on servers or to redistribute to lists, requires prior specific permission and/or a fee. Request permissions from Permissions@acm.org.

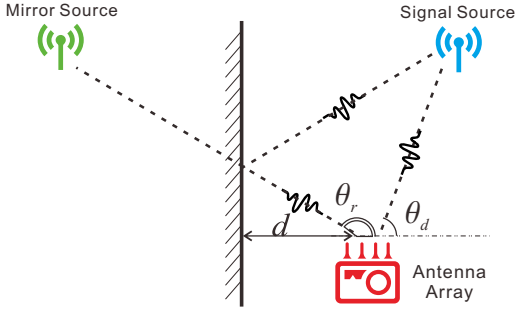
SenSys'14, November 3–5, 2014, Memphis, TN, USA.
Copyright 2014 ACM 978-1-4503-3143-2/14/11 ...\$15.00
<http://dx.doi.org/10.1145/2668332.2668345>

1 Introduction

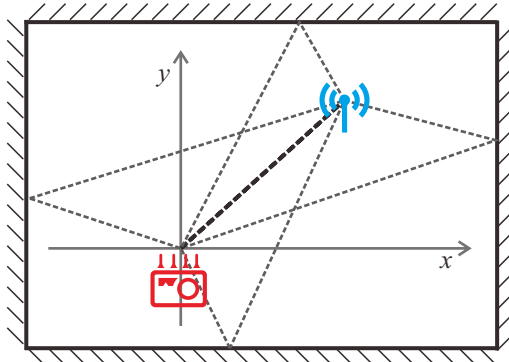
Since its inception in early this century (due to seminal work such as RADAR [1]), indoor localization has been one of the most important research topics in wireless system community. This is obviously driven by need from our real-life experience: finding where other people are and even oneself is in large scale indoor facilities (e.g., shopping malls or airport terminals) is becoming increasingly difficult due to the ever growing of our cities and thus their facilities. Unfortunately, technologies invented in the last decade all bear crucial weaknesses that prevent them from being put into practice. On one hand, RSSI-based ranging-trilateration methods (e.g., EZ [3]) may not scale to large indoor spaces as RSSI can be a bad indicator of distance due to multipath and shadowing. On the other hand, fingerprint-based approaches (e.g., Horus [26]) require expensive war-driving to set up a fingerprint map and are hence not adaptive to layout changes.

Recently, improving the aforementioned approaches using physical layer information has become a new trend [20, 6, 19]. In particular, both ArrayTrack [6] and CUPID [19] apply an array of antennas to estimate the Angle-of-Arrival (AoA) of the direct path, while CUPID [19] takes one step further by using Channel State Information (CSI) to get more accurate estimation of the path length. Synthesizing the estimations (AoAs or even path lengths) from a few sensors would allow for an accurate location estimation for the signal source. Interestingly, both ArrayTrack and CUPID treat reflection signal paths as “noises” and make great efforts to remove them, while they in fact contain valuable information. As illustrated in Figure 1(a), whereas the AoA of the direct path (θ_d) is what is sought by both ArrayTrack and CUPID, the AoA of the reflection path (θ_r), which was thrown away by the existing approaches, indicates the locations of a mirrored image of the signal source with respect of one wall. Given a known distance from the sensor (an antenna array)¹ to the wall, the source location can be estimated with θ_d and θ_r . In reality, multiple reflection paths do exist in an indoor space, as shown in Figure 1(b). Exploiting all these paths may allow us to learn not only the location of the source but also the geometry of the space, whereas this latter piece of information is missing in almost all indoor localization systems: a floor plan often needs to be known in advance.

¹We use “sensor” and “antenna array” interchangeably in our paper, as they refer to the same thing in our context.



(a) Direct path and one reflection path.



(b) Direct path and multiple reflection paths.

Figure 1. Multipath contains useful information.

Aiming at demonstrating that all these aforementioned multipath features can be actually put into use in assisting indoor localization, we construct an antenna array system, iLocScan, using multiple USRP2 Software Defined Radios (SDRs). iLocScan simultaneously samples the signals from its multiple antennas, and the samples are infused into a computation module running a fine-tuned version of MUSIC [18], in order to obtain a set of estimated AoAs (including both direct path and multiple reflection paths). iLocScan then uses a logic module to i) tell which AoA belongs to which path, if a sufficient number of AoAs have been gathered, and otherwise ii) suggest a possible new location to gather more AoAs. Finally, all the acquired information are put together to form a least squares problem that computes the estimations of various variables (including both source location and space geometry) as those best fitting the known parameters. Although our iLocScan prototype is designed to work with 2.4GHz WiFi signals, it has the potential to track most microwave signal sources, including mobile phones, ZigBee, and Bluetooth. In summary, we are making the following major contributions in implementing iLocScan and in understanding the features of indoor radio signal:

- We engineer iLocScan to fully exploit the power of multipath rather than to simply avoid it; this enables us to utilize far more information embedded in the radio signals propagating indoors.
- We, for the first time, design a system that can simultaneously locate a signal source and sketch the plan of the floor where the source is located at.

- We perform detailed experimental investigations on the performance of various antenna arrays and the properties of indoor multipath propagations of radio signal; the results not only guide us in designing iLocScan but also have the potential to benefit future developments.
- We implement iLocScan using several USRP2 units, and we perform extensive experiments on it in various indoor spaces. The results strongly confirm the feasibility of exploiting multipath for assisting indoor localization and for automatically constructing floor plans.

As iLocScan does not require any support from an already deployed infrastructure (e.g., a set of WiFi APs), it is very useful in venues where no infrastructure is available. Though the current prototype of iLocScan is rather bulky due to the large size of individual USRP2 units, our long term vista is to have it integrated into a hand-held device.

The rest of our paper is organized as follows. We first briefly describe the relevant problem scenarios and introduce the iLocScan architecture in Section 2. Then we present the three components of iLocScan respectively in Section 3, 4, and 5. We report the implementation details and field tests respectively in Section 6 and 7. We survey related literature and discuss some future directions in Section 8, before finally concluding our paper in Section 9.

2 Applications and System Architecture

We first explain the applications scenarios that drive our system design, then we give a general overview of the system architecture of iLocScan. We briefly discuss the design challenges behind each individual component, but leave the details to the later sections.

2.1 Finding Signal Sources Indoors

In most of the metropolitan areas, people keep building tremendous business and entertaining facilities (such as shopping malls, airport terminals, convention centers), and they do spend plenty of time inside such indoor spaces for both working and entertaining. However, the ever growing complexity of these indoor structures makes it increasingly troublesome for people to find where themselves are and also **where a person/object-of-interest is**. While the majority of the indoor localization proposals aim to handle the former problem (i.e., locating users themselves), we set about tackling the latter issue (i.e., finding someone of interest to a user). Imaging the scenario where a user walks into an indoor facility (say an airport terminal) wishes to find another person, as show in Figure 2, thus our goal is to development a device that helps the user to achieve this objective.

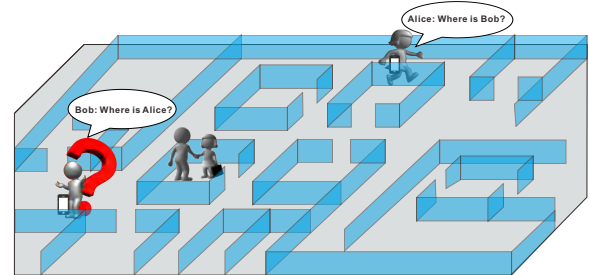


Figure 2. Searching for a person-of-interest indoors

Obviously, an existing indoor localization system can be a candidate solution, as the system keeps track of the location of every user in order to respond to the location queries from individual users. Unfortunately, it is not necessarily the best solution due to the following reasons. First of all, there might not be such a system deployed in the facility. Secondly, temporarily deploying such a system consisting of a collection of networked sensors² (e.g., [6, 19]) is too costly and may disturb other people. Thirdly, even if an indoor localization system is in position, the person/object-of-interest may not want to register to the system due to, for example, privacy concerns. Last but not least, majority of the proposed indoor localization systems require the floor plans to be ready.

In reality, the pervasive availability of wireless gadgets almost always makes every person a signal source: he/she might have a mobile phone, or might even have a device (the phone or a iPad) connected using WiFi. Assuming the device IDs are known, tracking the corresponding radio signals may reveal the locations of the sources. Albeit the similarity to shooter localization (e.g., [16]), positioning radio source indoors can be fundamentally different from locating acoustic source outdoors: the former has its specific challenges given the complicated indoor structures and the totally different signal propagation features between sound and radio signal. In particular, we may not afford to deploy a network sensing system given the reason discussed earlier.

The major obstacle that prevents us from building a simple yet fast source localization system is the limited information acquired by a single sensor: for example, ArrayTrack [6] only obtains the AoA of the direct path signal with respect to each sensor. Consequently, locating a signal source is possible only if a networked sensing system with multiple synchronized sensors is in position. Fortunately, radio signals propagating indoors contain far more information than those have been utilized. As illustrated in Figure 1, information buried in multipath, which used to be filtered but if properly utilized, may potentially suggest the location of the source, as well as the floor plan on which the source is. However, designing such a “two-bird one-stone” system is far from trivial. Whereas antenna arrays have been used recently to detect the AoA (and even length) of the direct path [6, 19], how to handle the reflection paths is still an open issue. Moreover, existing designs unanimously take a linear antenna array, but which antenna pattern suits the best for exploiting multipath is yet to be investigated. Finally, the system has to handle the situation where information at one spot is not sufficient, possibly due to the complicated indoor structures.

2.2 Our Solution: iLocScan

We hereby present iLocScan as a prototype for simultaneously indoor source Localization and space Scanning. In designing iLocScan, we intend to deliver some preliminary results to demonstrate the feasibility of harnessing multipath for liberating indoor localization from the reliance on any pre-deployed infrastructure. Although iLocScan may not achieve the centimeter level of localization accuracy as re-

ported in [6], the edge of iLocScan is very clear: it requires a single sensor (instead of multiple networked ones) and it does not demand the knowledge of the floor plans. The general system architecture is presented in Figure 3. Basically,

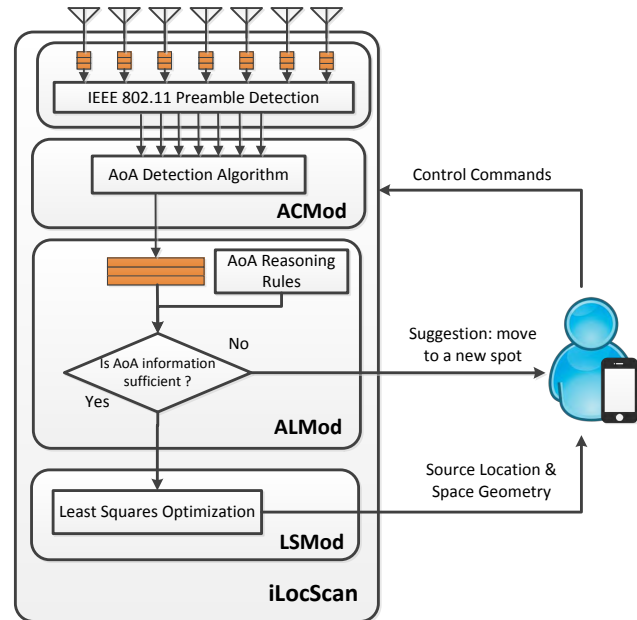


Figure 3. iLocScan architecture.

it has a *multi-input radio system with an antenna array* at its physical layer (the module at the top). The *AoA Computation Module (ACMoD)* takes the signals gathered by all the antennas to derive a set of AoAs. Then the *AoA Logic Module (ALMoD)* attempts to separate direct path from the remaining reflection paths. If it succeeds given a sufficient number of observed AoAs, the *Least Squares Module (LSMod)* will be invoked to estimate the source location, as well as the geometry of the space. Otherwise the logic unit will indicate a new spot, which may potentially yield sufficient AoA observations. In the following, we briefly discuss the challenges in designing these modules.

2.2.1 Antenna Pattern and AoA Estimation

As the physical component of iLocScan, the antenna array is crucial to the performance of our system. In particular, we are concerned with what antenna pattern to be used for detecting AoAs. Recent proposals only apply a linear array, but the aim of those proposals is only to identify the AoA of the direct path. As iLocScan needs to detect the AoAs of all directions along which the signal gain is significant, we need to compare various antenna patterns in terms of their ability in discriminating these AoAs. Assuming a system with 7 antenna, the following Figure 4 shows four meaningful patterns that we shall investigate.

Several mature algorithms can be applied to synthesize the readings gathered by multiple antennas and thus to estimate AoAs. Among them MUSIC [18] is popular as it entails a rather straightforward implementation. Although directly using MUSIC has been shown to be effective in identifying the AoA of the direct path [6, 19], certain fine-tuning has to

²Fingerprint-based systems (e.g., [26, 22]) are not very useful in this circumstance, as they often has a very long lead time required for constructing the fingerprint map.

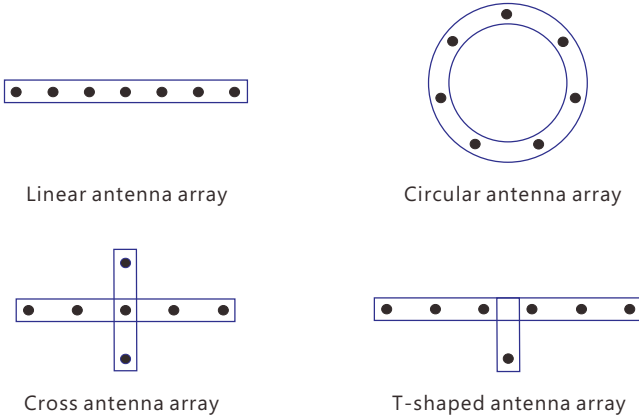


Figure 4. Four antenna patterns.

be applied to make MUSIC suitable for the ACMoD of iLocScan. Essentially, as the original MUSIC algorithm appears to be designed under an (implicit) assumption that the number of antennas is much larger than the number of incoming signals, applying it directly is fine for detecting only the direct path AoA, but may not be adequate for estimating all potential AoAs.

2.2.2 Extracting Information from AoAs

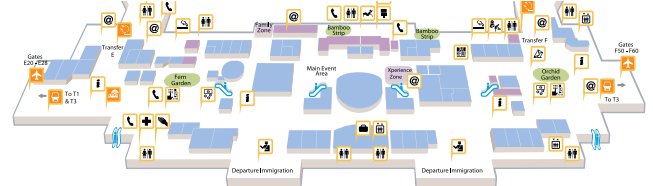
After obtaining a set of AoAs, the next crucial step is to tell the AoA of the direct path from others or, in the worst case, to tell whether this AoA exists or not. Existing approaches rely on either the stability of AoAs [6] or the mobility-induced AoA variance [19] to identify the direct path, but they are not suitable for the application scenarios targeted by iLocScan. On one hand, the stability criteria works only if there is a line-of-sight path between the signal source and iLocScan, which may not be the case initially. On the other hand, requiring mobility is not practical in our applications as the signal source is not controlled by our system. Therefore, iLocScan needs the logic module, ALMod, to reason about the geometry relations among different paths.

As illustrated by Figure 5(a), most indoor spaces have a rather regular layout. In order to facilitate the reasoning of AoAs, iLocScan assumes a simple yet powerful model for indoor spaces: an *axis-aligned* polygon shown in Figure 5(b).³ Under such a circumstance, ALMod mainly needs to reason about two typical situations: a rectangular area and an L-shaped area, as shown by the hatched areas in Figure 5(b): it determines which AoA is that of the direct path in the former case, while it simply senses the latter case and then suggests a new spot so that iLocScan may potentially get better readings in terms of AoA by moving there.

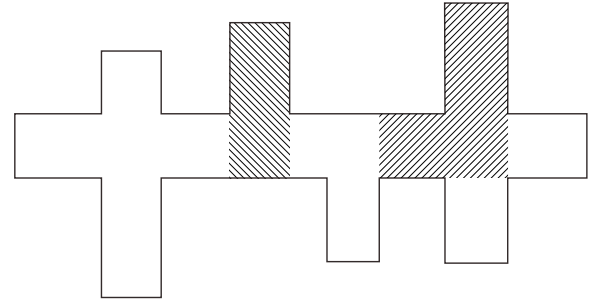
2.2.3 Simultaneous Localization and Mapping

After having a sufficient amount of information on the AoAs of various paths, LSMoD puts these constraints together to make an overdetermined equation system and try to estimate the variables (source location and space geometry). Solving this overdetermined equation system by minimizing the sum of the squares of the errors is a rather standard procedure, but we need LSMoD to autonomously build

³We shall discuss the extension to more general scenarios in Section 8.4.



(a) Floor plan of a typical airport.



(b) An axis-aligned model.

Figure 5. Indoor space model for iLocScan.

the optimization problem and then solve it. Whereas building an equation system automatically in general is far from trivial, we can take the advantage of the special structure of our problem and hence allow LSMoD to derive the model by itself. As an iLocScan user may need to collect information at different spots, the locations of these spots (relative to the initial spot) should be the input to LSMoD. We let the person who operates our iLocScan prototype to bring a mobile phone for this purpose: it measures the displacements using the dead-reckoning method reported in [24, 8].

3 ACMoD – Measuring All AoAs At Once

It is well known that microwave signal (including, for example, 3G, WiFi, and ZigBee) can be reflected by obstacles and thus creates multipath in an indoor space. Our iLocScan differentiates itself from existing proposals in its attempt to exploit the information inferred by multipath instead of simply filtering the reflection paths. In this section, we present the technical details of ACMoD (iLocScan’s module on estimating AoAs) by answering the challenges raised in Section 2.2.1. As some algorithm details have been discussed in [6], we focus on our fine-tuning of the algorithm, as well as experimental evaluation of the antenna patterns.

3.1 Preliminary on AoA Estimation

Most wireless communication systems are using QAM to modulate their signal, so our design is based on the assumption that each symbol carried by wireless signal has an I-Q representation. Typically, for a complex symbol with *amplitude* a and *frequency* f , it can be represented as

$$ae^{j(2\pi ft + \varphi)} = a \cos(2\pi ft + \varphi) + ja \sin(2\pi ft + \varphi),$$

where φ is the phase of the modulating symbol. On the I-Q plane, the symbol can be considered as a point rotating counter-clockwise around the origin, and $\Phi = 2\pi ft + \varphi$ denotes the *instantaneous phase*.

Denoting the distance from the source to the first antenna by d , the phase of the signal arriving at the receiver will be

$$\varphi_1 = 2\pi d\lambda^{-1} + \varphi$$

where $\lambda = c/f$ is the wave length of the signal, with c being the speed of light. Obviously, varying the distance d will change the phase of the received signal. Now let us take a second antenna whose distance towards the first antenna is \tilde{d} . Assuming the AoA of the signal with respect to the two-

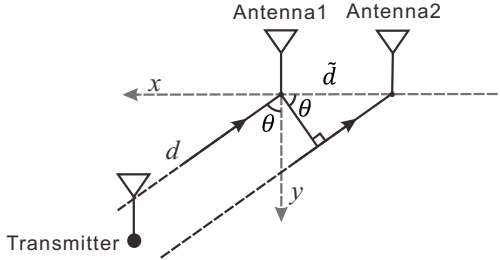


Figure 6. Detecting the AoA of a signal path using a two-antenna array. The antennas are aligned with the x -axis, while the y -axis indicates the forward direction, i.e., the detected AoA represents the signed angle counter-clockwise from y -axis to the signal's steering direction.

antenna array is $\theta \in (-\pi/2, \pi/2]$ and, without loss of generality, $d \gg \tilde{d}$, we may derive the distance from the transmitter to the second antenna as $d + \tilde{d}\sin\theta$. Consequently, there is a constant offset $\Delta\Phi = 2\pi\sin\theta\tilde{d}\lambda^{-1}$ between the instantaneous phases of the two antennas. To eliminate the ambiguity in computing this phase offset, the phase offset should be less than π . Typically, one may space the two antennas by half of the wavelength, i.e., $\tilde{d} = \lambda/2$, and thus $\Delta\Phi = \pi\sin\theta$. As a result, with a measurement of $\Delta\Phi$, we can derive the AoA as $\theta = \arcsin(\Delta\Phi\pi^{-1})$. Apparently, the $\Delta\Phi$ is independent of the signal amplitude a and symbol phase φ , so any symbol transmitted by WiFi can be used for the purpose of estimating AoA. Without loss of generality, we hereafter assume $a = 1$ and $\varphi = 0$ to simplify the exposition.

3.2 Fine-Tuning the MUSIC Algorithm

In reality, what each antenna receives is actually the superposition of several signals (from both direct and reflection paths) with different AoAs. To handle this, several algorithms have been proposed and among them MUSIC [18] is the most popular one. However, our experiments show that the original MUSIC algorithm does not perform very well when the number of antennas is not far beyond the number of signal paths. Therefore, we shall first introduce the basics of MUSIC, and then present our fine-tuning to the algorithm.

3.2.1 MUSIC Primer

Assume there are N antennas in the array, and signals from M directions are received by the antenna array. Obviously, N should be more than M for eliminating multi-path ambiguity. Since the signals are time varying, the input of the MUSIC algorithm is a set of signal samples taken at the N antennas at the same time. Denote by $\mathbf{s} = [s_1, s_2, \dots, s_M]^T$ the incident signal from M directions, $\mathbf{r} = [r_1, r_2, \dots, r_N]^T$ the signal vectors received by N antennas, and $\mathbf{w} = [\omega_1, \omega_2, \dots, \omega_N]^T$

the noise vector at the antenna array. The incoming signal of the i -th antenna can be defined as the combination of the M signals from different directions plus the noise

$$r_i = \sum_{k=1}^M g_i(\theta_k)s_k + \omega_i, \quad (1)$$

where $g_i(\theta_k)$ is the *gain* of the k -th signal received by the i -th antenna. Overall, \mathbf{r} can be characterized by the following linear model

$$\mathbf{r} = \mathbf{G}\mathbf{s} + \mathbf{w} \quad (2)$$

where $\mathbf{g}(\theta_k) = [g_1(\theta_k), g_2(\theta_k), \dots, g_N(\theta_k)]^T$ is the *steering vector* for the k -th signal and $\mathbf{G} = [\mathbf{g}(\theta_1), \mathbf{g}(\theta_2), \dots, \mathbf{g}(\theta_M)]$.

In order to estimate $\{\theta_k\}_{k=1, \dots, M}$ from the observed signal vector \mathbf{r} , MUSIC exploits the fact that the correlation among signals received at different antennas contains the information about the directions indicated by the steering vectors. Denote by \mathbf{C}_r the $N \times N$ *correlation matrix* of the received signal, we have, according to [18],

$$\mathbf{C}_r = \mathbf{G}\mathbf{C}_s\mathbf{G}^* + \sigma_w^2\mathbf{I}$$

where $*$ represents a conjugate transpose, \mathbf{C}_s denotes the correlation matrix of the incident signals, and σ_w^2 is the variance of the (zero mean and i.i.d.) noise. Apparently, $\mathbf{G}\mathbf{C}_s\mathbf{G}^*$ is singular and has a rank of M if the number of the incident signal is less than the number of the antennas (i.e., $M < N$). Therefore, if $\{\tau_1 \geq \tau_2 \geq \dots \geq \tau_N\}$ and $\{\mathbf{u}_1, \mathbf{u}_2, \dots, \mathbf{u}_N\}$ are eigenvalues and corresponding eigenvectors of \mathbf{C}_r , we have $\tau_{M+1} = \tau_{M+2} = \dots = \sigma_w^2$, and

$$\{\mathbf{u}_{M+1}, \mathbf{u}_{M+2}, \dots, \mathbf{u}_N\} \perp \{\mathbf{g}(\theta_1), \mathbf{g}(\theta_2), \dots, \mathbf{g}(\theta_M)\}. \quad (3)$$

In other words, the noise space $\mathbf{U}_n = [\mathbf{u}_{M+1}, \mathbf{u}_{M+2}, \dots, \mathbf{u}_N]$ is orthogonal to the column space of \mathbf{G} in an ideal case. However, this orthogonality may not hold strictly. Therefore, the original MUSIC algorithm proposes to scan the angle spectrum by computing

$$P_{\text{MU}}(\theta) = \frac{1}{\mathbf{g}(\theta)^*\mathbf{U}_n\mathbf{U}_n^*\mathbf{g}(\theta)} \quad (4)$$

The rationale is the following: if $\theta \in \{\theta_k\}_{k=1, \dots, M}$, P_{MU} would be rather large due to the orthogonality stated above.

3.2.2 MUSIC for *iLocScan*

As our later comparisons will show, running MUSIC to detect all AoAs leads to rather unstable results, i.e., the angle spectrum P_{MU} may differ significantly in time, thus affecting the accuracy of AoA estimations. In fact, according to the orthogonality condition in (3), we also have $\mathbf{g}(\theta_1), \dots, \mathbf{g}(\theta_M)$ exactly lying in the signal space \mathbf{U}_s spanned by $\mathbf{u}_1, \dots, \mathbf{u}_M$. In particular, $\mathbf{u}_1, \dots, \mathbf{u}_M$ are indicating the most correlated directions. Therefore, we redefine the angle spectrum as

$$P_{\text{iLocScan}}(\theta) = \mathbf{g}(\theta)^*\mathbf{U}_s\mathbf{U}_s^*\mathbf{g}(\theta) \quad (5)$$

Ideally, P_{MU} and $P_{\text{iLocScan}}(\theta)$ should be exactly the same. In reality, if $N - M < M$, \mathbf{U}_s contains more information; or the other way around if $N - M > M$. As an antenna array may not contain more than 8 antennas due to size limit while there could be up to 5 incident signals in an indoor environment, $P_{\text{iLocScan}}(\theta)$ (instead of $P_{\text{MU}}(\theta)$) should be used to improve

the accuracy of AoA estimations. Figures 7(a) and 7(b) compare the two angle spectrums under the same location arrangement (case): the spectrum generated by $P_{iLocScan}(\theta)$ is apparently more stable and hence yields a clearer indication of the AoAs. We also use Figure 7(c) to compare the stability of measurements taken by both algorithms in terms of the spectrum variance at certain AoAs under several cases: it is rather straightforward to see the advantage of our tuned MUSIC in having stable measurements.

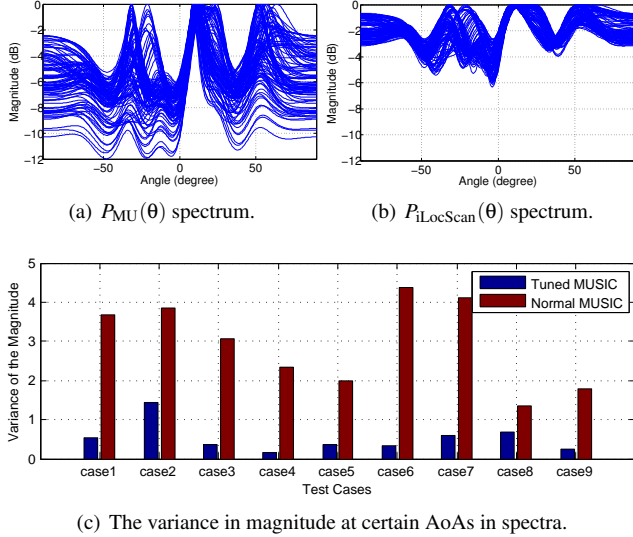


Figure 7. Comparing the normal and tuned MUSICs.

3.3 Antenna Patterns

A crucial component of iLocScan is its antenna array, as it determines the quality of information the system may acquire. Although several patterns are possible (shown in Figure 4), linear antenna array is often used in the literature for detecting the AoA of direct path. As our objective is to identify all possible AoAs, it is necessary to investigate the performance of these patterns experimentally. We apply our fine-tuned MUSIC algorithm to each of these patterns by adapting its steering vector. For example, the steer vector for linear array is $[e^{-j2i\pi \sin\theta d\lambda^{-1}}]_{i=0,1,\dots,N-1}^T$ (according to Section 3.1), and that for circular array is $[e^{-j2\pi \cos(2i\pi N^{-1}-\theta)R\lambda^{-1}}]_{i=0,1,\dots,N-1}^T$ with R being the circle radius, derived based on Figure 8.

One of the important metrics for an antenna array is its resolution: the minimum discernable angle difference between two neighboring AoAs. According to the statistics shown in Table 1, linear has the best resolution, but T-shaped is very close to it. This is obviously due to the fact that

Table 1. Angle Resolution of Different Antenna Arrays.

	Linear	Circular	Cross	T-Shaped
Min Angle Diff (degree)	18	24	34	21

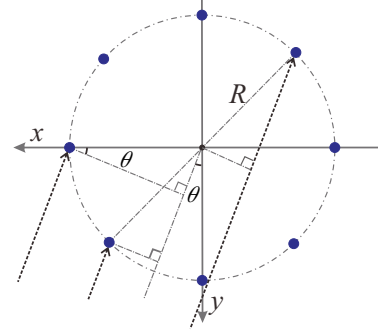


Figure 8. Circular antenna array. The blue points denoting the antennas are uniformly placed on a circle with radius R . The signal AoA is θ .

linear uses one more antenna to measure phase differences, whereas T-shaped has to partially sacrifice it for telling the sign of an AoA⁴. We also illustrate in Figure 9 the same three AoAs recognized by different antenna arrays.

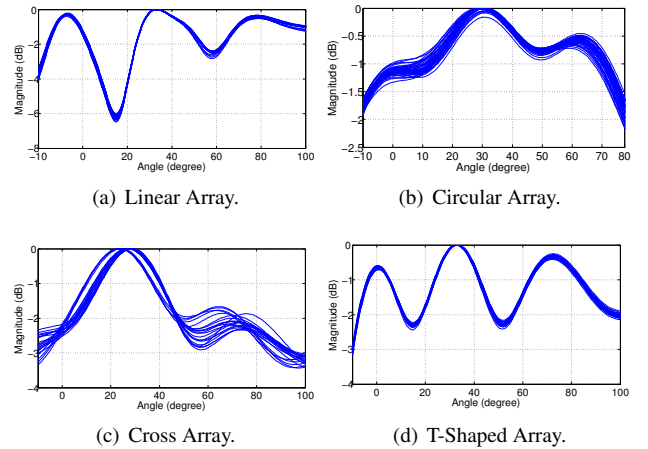


Figure 9. Angle spectra of different arrays.

Another related metric is the accuracy of measuring angles. We plot the CDF of angle error results from different arrays in Figure 10. It is clear that the T-shaped array performs the best; this seems to be related to the rather regular spectrum produced by it compared with others, as shown in Figure 9. As the linear array is a 1D pattern, it has a border effect: AoAs close to zero degree may not be measured accurately. Other 2D patterns avoid such negative effect, but offers lower resolution. Therefore, our results advocate T-shaped array: it retains the good properties of linear array while avoiding its drawback. When using the linear antenna array in later experiments, we take two measurements at one spot, with antenna directions perpendicular to each other. This allows the linear array to obtain much better accuracy than others (as it yields more readings at one spot), but at the cost of a higher system latency.

⁴According to the discussion in Section 3.1, a 1D array cannot distinguish AoAs in $[-\pi/2, \pi/2]$ from those in $(-\pi, -\pi/2) \cup (\pi/2, \pi]$.

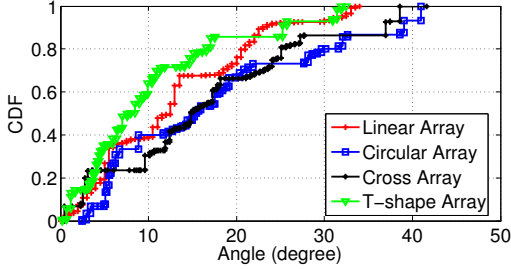


Figure 10. Accuracy of angle measurement by different arrays.

4 ALMod – AoA Reasoning

Given AoAs measured by ACModule, we need ALMod to extract information from these measurements, and also to determine whether further information is needed. According to the axis-aligned model discussed in Section 2.2.2, this reasoning proceed boils down two specific cases: rectangular area and L-shaped area. In the following, we first discuss the basic rules that ALMod applies to reason AoAs in a rectangular area, then we introduce the algorithm to perform localization and scanning in a complicated indoor space.

4.1 The Case of A Rectangular Area

As discussed in Section 2.2.2, indoor layouts are often axis-aligned from a geometric point of view. In particular, the most elementary unit is a rectangle area whose sides are aligned with the axes of the coordination system. Therefore, we first study this basic case where both iLocScan and the signal source are placed inside such a rectangular area with all four sides being able to reflect the signals. We also assume the axes of iLocScan are aligned with those of the area.

Our experiments in such a cell show that, except for direct path signal, only single-reflection signals are strong enough to be detected by ACMod, whereas those multiple-reflection ones usually have far less strength and thus may not be sensed. Under such a circumstance, ACMod should be able to detect up to five AoAs, and observing the distribution of the detected AoAs in the four quadrants would allow ALMod to figure out which one is the direct path. The following are the reasoning rules:

- **5-AoA:** We refer back to Fig. 1(b) for an illustration of such a case. Basically, there is always one quadrant containing three AoAs, so the one in the middle corresponds to the direct path: *middle rule* hereafter.
- **4-AoA:** These are degenerated cases where exactly one of the following three conditions holds:
 - C1: iLocScan and the source are co-linear along one axis: Figure 11(a).
 - C2: The source is close to one side: Figure 11(b).
 - C3: iLocScan is close to one side: Figure 11(c).
 The consequence is that three AoAs are separated from the fourth by one axis, so the middle rule applies.
- **3-AoA:** These are degenerated cases where two or more of the C1–C3 hold, as shown by Figure 11(d)–(h). Note that this includes the case where the same condition

holds twice, i.e., C2 is satisfied twice infers that the source is at a corner: Figure 11(d). For the cases shown by Figure 11(d)–(e), the AoA in the middle still corresponds to the direct path. However, we cannot draw a right conclusion due to the ambiguity introduced by Figure 11(f)–(g). Fortunately, we may break C3 by moving iLocScan away from the side, which would allow a right conclusion to be drawn. As for Figure 11(h), a *side rule* applies: the AoA aligned with one axis and on the majority side corresponds to the direct path.

- **2-AoA:** This is a very special case where both C2 and C3 hold and one of them holds twice, as shown by Figure 11(i). For this case, ALMod would again suggest breaking C3. The case of 1-AoA shown in Figure 11(j) is similar to the 2-AoA case.

In summary, ALMod should be able to identify the direct path using the middle rule under both 5-AoA and 4-AoA cases. If less AoAs are detected, ALMod check if C3 holds (which requires user confirmation). If false, the middle rule still applies; otherwise ALMod alerts the user to break C3.

4.2 A Rectangular Area with Open Side(s)

This case is similar to the closed area case, if we add a “virtual wall” on the open side and deem the object (iLocScan or the source) closer to the open side as being “on the wall”. This implies that either C2 or C3 always holds. Under this circumstance, 5-AoA does not exist, but all 4-AoA cases still allow the middle rule to be applied. However, a user cannot break C3 anymore, leaving the ambiguity between Figure 11(f) and (g) unsolvable. Nevertheless, the later LSMod should be able to find contradiction among one of the possibilities. For example, if the middle rule is applied to Figure 11(g), the area computed by LSMod will not be axis-aligned. As for the 2-AoA and 1-AoA cases, the strategy is to meet C3 by moving iLocScan, hence converting all such cases to Figure 11(h).

4.3 The L-Shaped Area and Beyond

Given a general axis-aligned polygon (see Figure 5(b)), there is yet another element differing from the rectangular area: the L-shaped area. Obviously, if ALMod handles both situations, it works for any general axis-aligned polygon spaces, as they can always be reduced to a combination of multiple L-shaped areas. Therefore, we hereby discuss how ALMod copes with an arbitrary L-shaped area. When iLocScan and the source are not co-located in the same branch of the L-shaped area, none of the above cases apply. The strategy taken by ALMod is to move iLocScan such that we may get back to the rectangular area case. As shown in Fig. 12,

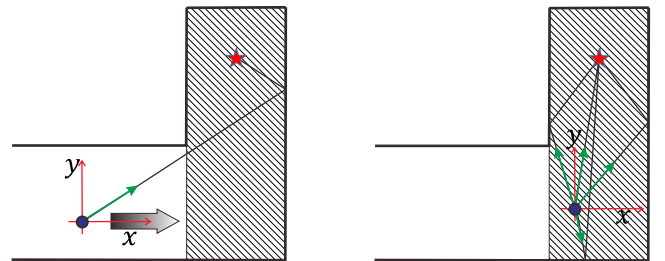


Figure 12. L-shaped indoor structure.

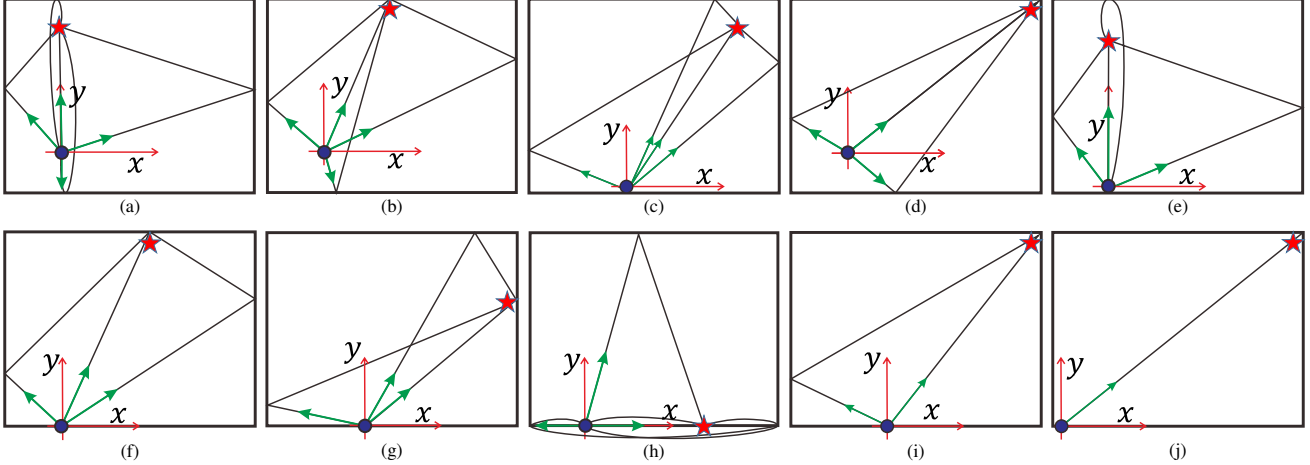


Figure 11. AoA patterns. We denote iLocScan and the signal source by blue dot and red star, respectively. We also mark the coordinate system of the antenna array by red arrows, and the detected AoAs by green arrows.

when all AoAs point towards the positive direction of the x-axis which also implies the location of the signal source in some extent. We then move our antenna array along the positive x-axis towards the hatched area until our antenna array reaches the same rectangular area as the signal source; this brings the situation back to what has been discussed in Section 4.2. Essentially, ALMod applies a *coordinate-wise searching* method, and always moves iLocScan along one axis directed by the AoA measurements.

5 LSMod – Autonomous Scenario Modeling and Problem Solving

With the information extracted by ALMod (probably after a few movements of iLocScan), it is now ready for LSMod to simultaneously perform source localization and sketching the indoor structure. The general principle behind LSMod is to form and then solve a least squares problem so that we fit the variables to be estimated to the measured AoAs. While forming and solving such a problem is rather standard for a human user, we would like the computing system to automatically complete the whole procedure.

Without loss of generality, LSMod takes the initial spot of iLocScan to be the origin of its global coordinate system. Remember iLocScan also has a local coordinate system, used by its antenna array, for measuring AoAs. The axes of both coordinate systems are aligned, but the local one always has the origin at the center of the antenna array. Also note that the user of iLocScan has to (visually) guarantee that the axes of iLocScan are aligned with those of the targeted indoor space. In Fig. 13, we use X - Y to denote the global coordinate system, and x - y to denote the local coordinate system. In the figure, we take a closed rectangular area as an example, whose four sides, under X - Y , can be expressed by $\Omega = \{\Omega_1 : x = w_1, \Omega_2 : y = l_1, \Omega_3 : x = -w_2, \Omega_4 : y = -l_2\}$ where $w_1, w_2, l_1, l_2 > 0$. Also, the unknown location of the signal source is $p = (x_p, y_p)$. The functionality of the LSMod is to determine these variables.

As iLocScan may need to visit more than one spot in order to acquire sufficient AoA information, we denote by $\hat{\theta}_i$

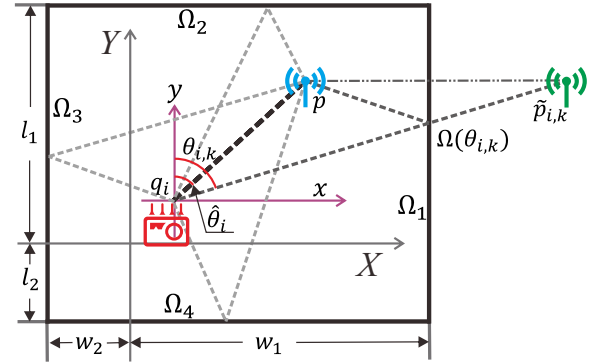


Figure 13. Illustrating automatic problem formulation.

the direct path AoA and by $\mathcal{A}_i = \{\theta_{i,1}, \dots, \theta_{i,k}\}_{1 \leq k \leq 4}$ the set of the reflection path AoAs, in the i -th measurements at spot $q_i = (\tilde{x}_i, \tilde{y}_i)$. For any $\theta_{i,k} \in \mathcal{A}_i$, its reflection wall is denoted by $\Omega(\theta_{i,k}) \in \Omega$. As iLocScan is using dead-reckoning to estimate the location of later spots relative to the initial one, $q_i = (\tilde{x}_i, \tilde{y}_i)$ is the input to LSMod. Now LSMod can express the AoA-side relationship as follows:

$$\cos \theta_{i,k} = f_{i,k}(p, w_1, w_2, l_1, l_2 | q_i) = \frac{(\tilde{p}_{i,k} - q_i) \cdot e_y}{\|\tilde{p}_{i,k} - q_i\|_2} \quad (6)$$

where e_y is the unit vector along the positive direction of Y -axis, $\|\cdot\|_2$ denotes the Euclidean norm, and $\tilde{p}_{i,k}$ indicates the mirror source of the targeted signal source with respect to $\Omega(\theta_{i,k})$; it can be represented in terms of p and coordinate of $\Omega(\theta_{i,k})$. Moreover, LSMod introduces the following equation for the direct path AoA $\hat{\theta}_i$:

$$\cos \hat{\theta}_i = f_i(p | q_i) = \frac{(p - q_i) \cdot e_y}{\|p - q_i\|_2} \quad (7)$$

Based on sufficient AoA observations, LSMod can now

formulate a least squares problem:

$$\begin{aligned} & \underset{x_p, y_p, w_1, w_2, l_1, l_2}{\text{minimize}} && \sum_i \sum_k (f_{i,k} - \cos \theta_{i,k})^2 + \sum_i (f_i - \cos \hat{\theta}_i)^2 \quad (8) \\ & \text{subject to} && -w_2 \leq x \leq w_1 \\ & && -l_2 \leq y \leq l_1 \\ & && z, w_1, w_2, l_1, l_2 \geq 0 \end{aligned}$$

where $\{x_p, y_p, w_1, w_2, l_1, l_2\}$ are the variables. We apply the *Trust-Region-Reflective* algorithm [4] to solve this optimization problem with bound constraints. As the dimension of the problem depends on the number of walls in an indoor space and the number of signal sources to be located, the problem cannot be of very large scale, as we normally aim at finding a few sources in a space with tens of walls. Therefore, solving this optimization problem does not lead to a significant overhead in computing.

6 Implementation Details

In this section, we present the technical details on the construction of our iLocScan prototype. In a nutshell, our hardware platform is based on USRP N210 (hereafter USRP2), while the software part, including ACMod, ALMod and LSMod, is implemented using Python and C++ under GNU Radio on a host computer.

6.1 A Multi-Input Radio System

The physical layer of iLocScan is a multi-input radio consisting of seven USRP2 units shown in Figure 14(a). Each USRP2 unit is equipped with an RF front end: an SBX daughter board and an omnidirectional antenna. These RX USRP2 units are controlled by a host computer through a Gigabit Ethernet switch, by which the signal samples taken by the RX USRP2 units are fed back to the software modules running on the computer. Additionally, the RX USRP2 units synchronize their native clocks through a common reference of 10 MHz and 1 PPS generated by an external clock, such that they can sample the incoming signals exactly at the same moment. Figure 14(b) shows the physical construction of iLocScan. We use a double-deck trolley to hold the system for free movements. The USRP2-based antenna array is put at the upper deck, along with the external clock and the reference signal source (see Section 6.2 for details). The lower deck holds the Ethernet switch. As this construction has to be powered; it has limited our choices of testing sites to a few research labs (rather than going to the real-life indoor spaces such as a shopping mall). Fortunately, it is possible to integrate this system onto a chip in the future, as the distance between neighboring antennas only needs to be a positive value below half a wavelength.

6.2 Phase Calibration

Only synchronizing the native clocks of the RX USRP2 units is not sufficient for our application, due to the random phase shifts caused by the radio's *Phase Locked Loop* (PLL) during the *Digital Down Conversion* (DDC) at each RF front end. These unknown phase shifts are added to the signal phases and thus may cause large estimation errors in ACMod's AoA detection procedure. To calibrate the RF front ends, we employ a reference USRP2 unit to transmit calibration signal (e.g., a 2.4 GHz sinusoidal carrier) to the

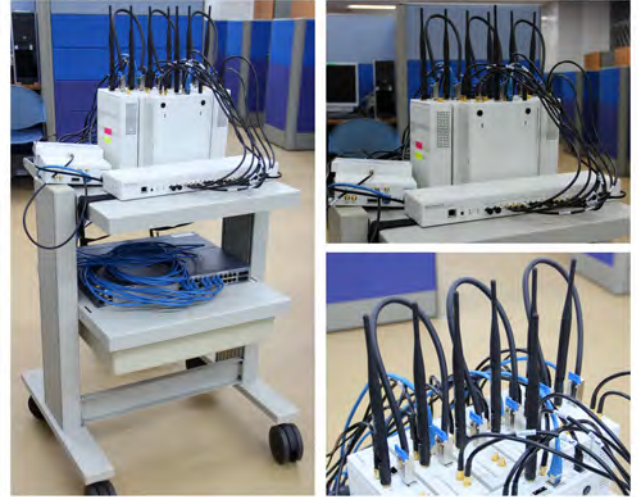
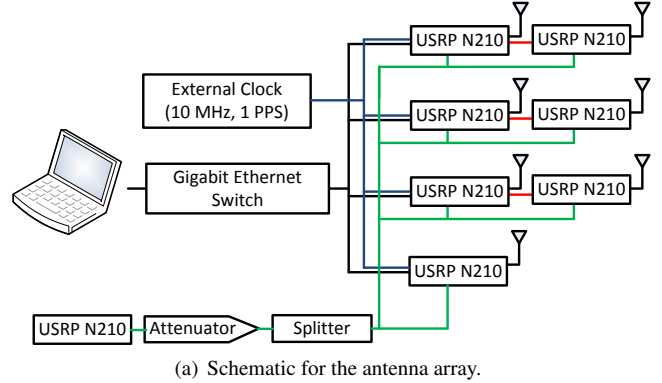


Figure 14. System schematic and outlook of iLocScan.

RX USRP2 units through a SMA splitter. Because all the RX USRP2s are connected to the SMA splitter via cables of equal length, the incoming calibration signal at each USRP2 device has the same phase. Let us denote by φ_{ref} and $\tilde{\varphi}_i$ the phase of the incoming calibration signal and the phase of the signal sample at the i -th RX USRP2 unit, respectively. Then the phase shift caused by DDC at the i -th RX USRP2 unit is $\tilde{\varphi}_i - \varphi_{ref}$. As the AoA measuring procedure run by ACMod is concerned with only the relative phase offsets between the RX USRP2 units, we simply need to align the phases of the RX USRP2 units to one of them (e.g., the first RX USRP2 unit). In particular, we can calibrate the i -th RX USRP2 units by subtracting $\tilde{\varphi}_i - \tilde{\varphi}_1$ from its signal sample, where $i = 1 \dots 7$.

6.3 Detecting WiFi Preamble

To acquire the bearing information of the targeted signal source, our ACMod needs to overhear the wireless communication originated from the source. As data packets are rather arbitrary and hence hard to control, we turn to the frame preamble. Each IEEE 802.11 frame starts with a short preamble sequence consisting of ten identical short training symbols with duration $0.8 \mu\text{s}$ each. The short preamble is often fairly robust and stable, so it serves as a good source of input to ACMod. Besides, as the USRP2 unit has a max-

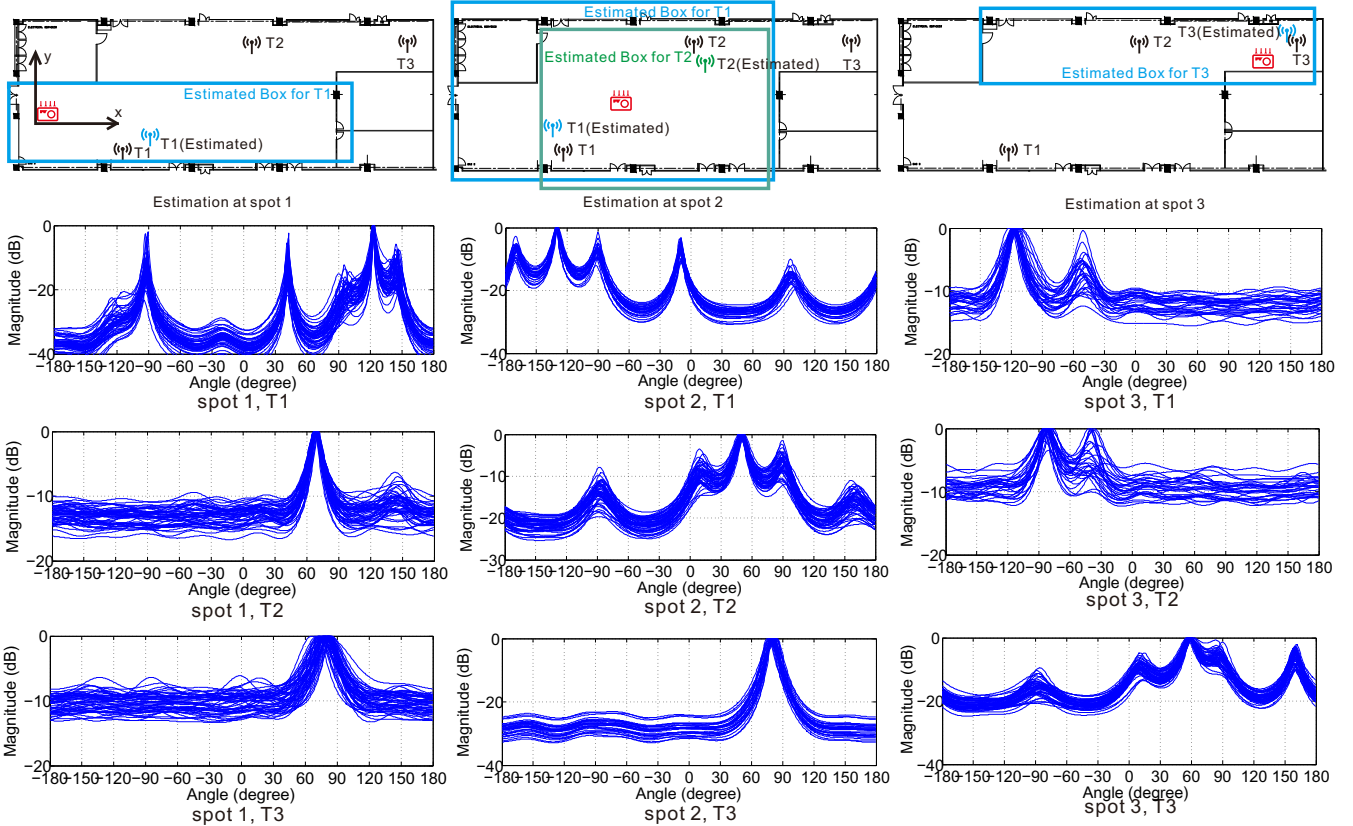


Figure 15. An illustration of iLocScan evaluation. This set of experiments is conducted in an 800 m² research lab. We fix three signal sources at location T1 , T2, T3. Our iLocScan chooses three spots to perform AoA measures. Each column of the figures corresponds to one iLocScan spot. The top row marks the measurement sports and also shows the estimated source locations and the floor plans. Another three rows plot the AoA measures for individual signal sources.



Figure 16. Test site (the 800 m² research lab) at a glance.

imum sampling frequency of up to 100 MS/s, this implies that it spends only 100 ns to take a sample from the incoming signal stream, sampling the short preamble sequence should be sufficient for the MUSIC algorithm as well as our fine-tuning version. We implement the preamble detection algorithm [17] in ACMod to extract the short preamble signals from the 802.11 frames. In particular, we set a buffer at each USRP2 unit’s frond end. Once the short preamble sequences are detected in all of the buffers, the samples will be delivered to ACMod. In our implementation, we take 30 samples from each preamble for ACMod to perform AoA detection, which is shown to be adequate to suppress noise and to ensure the estimation accuracy.

7 Experimental Evaluations

We have conducted extensive experiments with our iLocScan prototype at multiple test sites to verify its efficacy and robustness. In this section, we first briefly discuss the experiment settings, then we report the results on evaluating iLocScan. As a byproduct, we also obtain a large amount of data on the reflection properties of various indoor structures, which deliver insights that can be useful for the future developments of indoor radio sensing systems.

7.1 Experiment Settings

We perform many tests in three research labs; the floor plan of one of them is shown in Figure 15 (top row). Taking the advantage of having the digitized floor plans of these test sites, we can accurately design the ground truth locations of the signal sources to be located, and we also have accurate measurements of the geometry of these sites. We use three WiFi APs to emulate the signal sources, and we fix their locations in each of the test sites. In order to distinguish among these APs, we implement a full WiFi receiver functionality on our iLocScan prototype such that the APs are identified according to their SSIDs. As our iLocScan is movable, we often perform the initial measurements close to the entrance, and then choose new spots (if necessary) following the method discussed in Section 4.3. At each spot, iLocScan

may at most detect 5 AoAs for a given AP; this may not be sufficient to achieve accurate estimations. Therefore, we often take two observations at each spot, by moving iLocScan slightly off the spot for one meter. To keep track of the location of iLocScan, we employ a well-studied dead-reckoning scheme using inertial sensors in a smart phone [8]. Although the performance of dead-reckoning is subject to error accumulation in inertial sensing, our experiments are not affected by it due to their relatively small scales. Nonetheless, this is an issue demanding further studies.

7.2 A Concrete Example

Before diving into the statistical evaluations on the measurement accuracy of our iLocScan, we first use a concrete example to introduce how iLocScan prototype works in a real-life scenario and how the measurements have been obtained. As shown in Fig. 15, three targeted signal sources T1, T2 and T3 are placed arbitrarily in an S-shaped axis-aligned room, and they all operate on WiFi Channel 6. Recall that these WiFi APs are using CSMA mechanism to avoid interfering each other, so they do not transmit simultaneously. Consequently, the angle spectrum measured by iLocScan at given point in time corresponds only to one AP; this enables iLocScan to obtain three separated angle spectra shown in Fig. 15 (the lower three rows). The figures at the top row are illustrative, so measurement errors demonstrated in them are rather rough. We also provide a photo in Figure 16 for part of this axis-aligned room (the entrance part). In order to avoid the interference of the cubicles, we raise the height of iLocScan so that the antennas are higher than the cubicles.

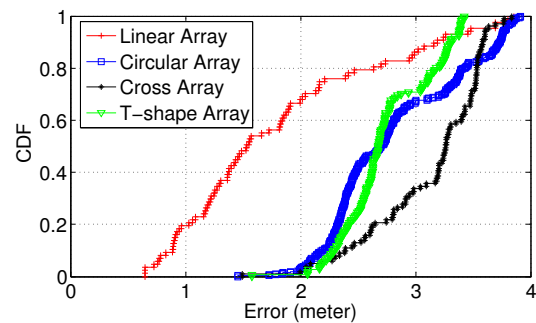
As shown in the first column of Fig. 15, our iLocScan starts to measure AoAs right after entering the space. It detects five AoAs from T1, but only one AoA from T2 and T3⁵. The AoA information collected at the first spot is sufficient to locate T1 and to estimate the geometry of the area marked by the blue box (which is only a partial view of the whole floor plan with some virtual wall being introduced). We then move iLocScan forward along the direction suggested by the detect AoAs of T2 and T3, as shown by the second column of Fig. 15. In the second spot, iLocScan can detect five AoAs for both T1 and T2, but still observes only one AoA for T3. This allows iLocScan to estimate the location of T2, as well as the two areas marked in blue and green. Combining the estimated geometry from the first two spots, the left side of the floor plan has now been fully constructed. The further collected AoA information on T1 can be used to refine the localization results we have obtained. Thanks to the direction implied by the AoA of T3, we move the iLocScan to the third spot shown in the third column of Fig. 15. At this spot iLocScan finally detects five AoAs from T3; it is hence able to locate T3 and to construct the full floor plan.

7.3 Accuracy Evaluations

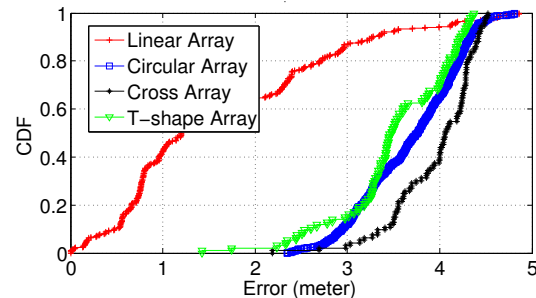
We first report the measurement accuracy by comparing our estimations with the ground truth. For localization accu-

⁵As discussed in Sec. 7.1, we need two observations at a give spot to achieve better estimations. Due to the space limitation, we only show the angle spectrum results of the first observation. Note that we plot 38 snapshots to demonstrate the stability of observed angle spectra, although it takes only one snapshot for iLocScan to detect these AoAs.

racy, the metric is the commonly used square-root error. For the floor plan geometry, the error is the distance shift of an estimated wall. As our floor plan model and the ground truth are both axis-aligned polygons, the estimation errors are only in the form of distance shifts. As shown in Figure 17, the localization error is less than 4 meters and the geometry error is less than 5 meters for all antenna patterns. Such an estimation accuracy is satisfactory in practice. Linear array (maximum error 3 meters and median error 1.9 meters in localization) performs far better than others simply because we take two perpendicular observations right at each spot (see Section 3.3 for details). This shows that, with linear array, we can trade detection latency for higher accuracy. Within the remaining three patterns, T-shaped array appears to have slightly better performance than the others, for the reason that have been studied in Section 3.3.



(a) Source localization error.



(b) Floor plan geometry error.

Figure 17. Evaluation of measurement accuracy.

As we have shown in Section 7.2, it is possible that iLocScan cannot locate the targeted signal sources and scan the floor plan fully with only a couple of spots. Using the large amount of data we have collected by randomly putting the WiFi APs in the three test sites, we show the chance of locating signal sources as an increasing function of the number of spots visited by iLocScan in Figure 18. Clearly, whereas one spot only allows less than 40% of the WiFi APs to be localized, almost all APs become localizable with up to 4 spots: the small fraction of non-localizable APs are at some corners, but the lab facilities prevent us from locating iLocScan properly (see Section 4.1 for details).

Normally, we take two observations per spot; this is how we obtain all the aforementioned results. One may wonder if adding more observations (at the same spot but slightly shifted from each other) would lead to higher accuracy. We

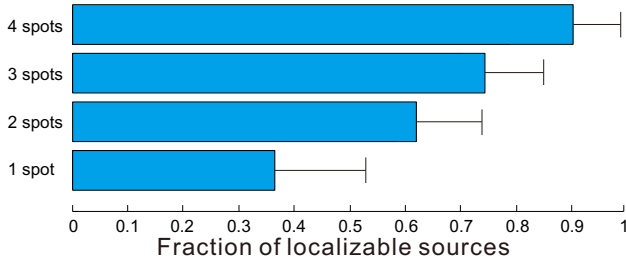
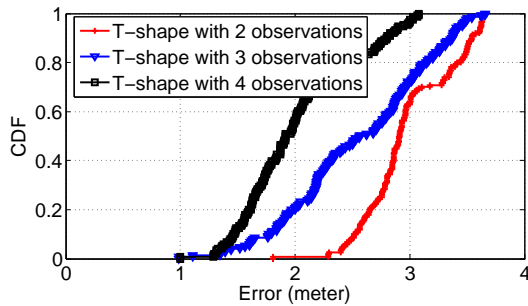
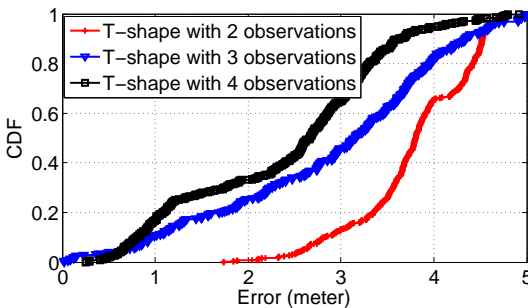


Figure 18. More spots yield higher chance of locating a source.

answer the question by showing more accuracy results in Figure 19. Apparently, the answer is yes, but at the cost of spending more time on the same spot.



(a) Source localization error.



(b) Floor plan geometry error.

Figure 19. More observations lead to higher accuracy.

7.4 AoA Detection under Varying TX Powers

We aim to design iLocScan to be compatible with a variety of wireless devices, which may have considerable heterogeneity, for example, in terms of tx power. Therefore, we now evaluate the robustness of iLocScan with respect to AoA detection in face of varying tx power. We set up one extra USRP2 unit to emulate a WiFi AP in our research lab and tune its output power from -80 to -40 dBm⁶. We perform twenty AoA measures under each tx power setting at a fixed spot 5 meters away from the WiF AP; the results are reported in Fig. 20. With extremely low tx powers (-80 to -70 dBm), the angle spectra are quite unstable so that it is rather difficult to estimate AoAs out of them. Further increasing the tx power to -60 dBm significantly stabilizes the angle spectra,

⁶A normal WiFi AP has a tunable tx power range around 10dBm, which is not low enough to test iLocScan in extreme cases.

but only with -40 dBm tx power iLocScan may detect all the three available AoAs. This set of tests suggest that increasing tx power affects the AoA detection in two ways: stabilizing the angle spectrum and improving the AoA resolution. As -40 dBm is still very low compared with normal WiFi tx power range, the ability of iLocScan to detect the reflection paths under this very low tx power has firmly demonstrated its applicability to real-life scenarios.

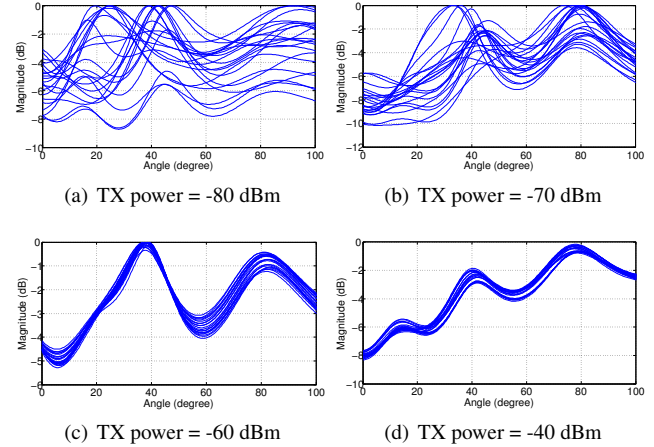


Figure 20. Angle spectra under different tx powers of the signal source.

7.5 Reflections on Different Materials

Today's indoor space may be constructed or separated by various materials. Though it is well known that, given a signal with certain frequency, different materials exhibit diverse reflection ability. Although this is currently not the main issue concerning the design and evaluation of our iLocScan, the large amount of data we have gathered while testing our system do allow us to shed some light on it. During our extensive tests, we have come across quite a few different building materials. For example, internal walls are often made of concrete, but wall facing outside can be made of glass. Moreover, metal boards can be used to separate a big hall into small rooms. Due to space limit, we only report a few typical results in Fig. 21. The reflection abilities of the three materials can be derived by comparing the magnitudes of the direct path signal with those of the reflection paths. We have observed that, among the three materials, metal has the strongest reflection ability as the reflection path signal may reach the same strength as the direct path signal, whereas the remaining two are comparable in terms of reflection ability. However, as glass is smoother than concrete on surface, the reflections tend to be slightly more stable.

In general, the reflection abilities of most indoor materials are sufficient for our iLocScan system to detect reflection path AoAs. However, knowing these properties may allow iLocScan to be better aware of the surrounding environments: it may not only estimate the geometry of an indoor space, but also figure out how it was constructed. As we shall discuss in Section 8.4, we are planning to modify iLocScan into a pure scanning device such that, without a few already deployed WiFi APs in a building, we may build the floor

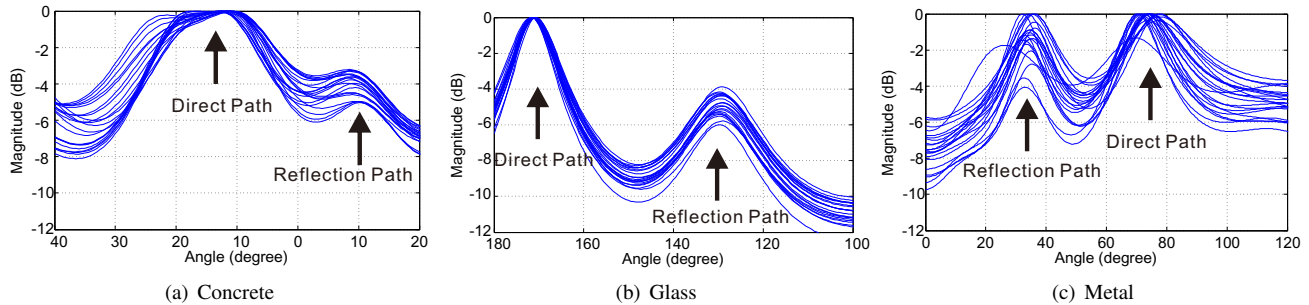


Figure 21. Reflections on concrete wall, glass window, and metal board.

plans automatically. We also notice that antenna polarization affects signal reflections, and iLocScan works well with vertically polarized waves. This is fortunately the situation for many real-life applications.

8 Related Work and Discussions

Though a large amount of indoor localization systems have been proposed in the last decade, they can be roughly categorized into two types: range-based [3, 10, 7] and fingerprint-based [26, 13, 22]. Recently, the performance of both types have been elevated by exploiting physical layer information [20, 6, 19]. Although these systems all bear in mind a rather different application scenario from ours and none of them has made efforts to exploit multipath, they still serve as motivation to our developments. In addition, we briefly discuss some potential directions along which our iLocScan can be further developed.

8.1 Range-based Indoor Localization

This category includes any methods that involve measuring distance, so it, in a sense, contains AoA-based methods, because AoA is measured through a combination of ranging and trigonometry. Earlier ranging techniques are mostly RSSI-based and were used for outdoor environment [23]. They were later adapted to indoor localization [9]: as indoor signal propagation is far more complicated than outdoors, the proposal requires to deploy a set of calibrated anchors to better characterize the relation between the RSSs. The same approach was later improved by using a mobile anchor that may sporadically get a GPS location fix indoors [3]. Though Time-of-Flight (ToF) can be a good indicator of distance, extremely accurate clock is needed to measure RF ToF [27], unless one replaces and complements RF with acoustic signal or ultrasound [12, 10, 7]. Time-of-Arrival (ToA) and Time Difference of Arrival (TDoA) can also be used for ranging, but earlier technology only allows them to be measured for acoustic signal or ultrasound [11]. In theory, TDoA can be translated to AoA through the induced phase difference (see Section 3.1), and a system that derives AoA from WiFi signal has been implemented only recently [25].

8.2 Fingerprint-based Indoor Localization

Compared with range-based approaches, this category appears to be more prosperous, probably due to the higher localization accuracy it may deliver in earlier stage [1]. Since RADAR [1] first performed detailed site survey to build a fingerprint map based on measured RSSI, a large amount of

proposals appeared and took various approaches to improve this method: Horus [26] applies a probabilistic approach to improve the localization accuracy based on WiFi fingerprint, while other proposals suggest to use different ambient signals as fingerprints, e.g., light intensity [15] and geomagnetic field [28]. In general, these approaches may suffer from the “curse” of wardriving [22], so several later proposals all aimed to handle this aspect. Redpin [2] allows users to identify location themselves when they are wrongly located and hence to correctly associate fingerprints to these locations. OIL [13] applies a similar approach to Redpin, but it further handles spatial uncertainty and labeling errors made by users. Zee [14] uses particle filter and dead reckoning to identify users walking trace and enriches the fingerprint database with the WiFi data collected along the trace. ARIEL [5] differentiates rooms through clustering on WiFi fingerprints collected by randomly moving users.

8.3 Exploiting Physical Layer Information

In recent years, researchers have started to exploit the fine-grained physical layer information to improve the performance of both categories. In particular, PinLoc [20] applies high resolution CSI fingerprints to combat the instability RSSI fingerprint, at the cost of higher complexity in constructing a fingerprint map. Both ArrayTrack [6] and CUPID [19] use an antenna array to estimate the AoA of the direct path, and CUPID [19] further performs ranging using CSI. As they both remove the reflection signal paths, the limited information acquired by each antenna array entails a set of such arrays whose individual measurements can then be synthesized to reach a location estimation for the signal source. Although the theoretical bounds of exploiting multipath have been recently studied [21], our iLocScan is the first system prototype to realize such ideas in the 2.4GHz band.

8.4 Potential Future Developments

Our current iLocScan prototype is designed to trace only WiFi signals, but its application scope should be broader than this. As other microwave signals do share the similar propagation features as WiFi signals, iLocScan should have the potential to locate devices emitting those signals. We are on the way of engineering iLocScan to handle 3G/4G and ZigBee signals so that it may locate person/object-of-interest equipped with other types of radios.

Another interesting aspect of iLocScan is its ability to build a floor plan using the measured AoAs. As roughly illustrated in Figure 15 (the top row), with three fixed WiFi

APs, moving iLocScan to three spots can sketch the S-shaped floor plan. In fact, most existing indoor localization systems simply assume the floor plans are available, but it is rarely the case in reality. So we are planning to extend iLocScan so that, with a few already deployed WiFi APs in a building, iLocScan can build all floor maps automatically. Potential challenges (also valid for iLocScan itself) are i) to handle floor plans beyond the axis-aligned model, and ii) to deal with the interference from moving crowd. A possible solution to i) is to model any non-axis-aligned walls as 45° slanted ones and absorb the incurred errors into the angle measurement errors of the antenna array. The temporary makeshift that we adopt currently to tackle ii) is to take a sequence of measurements at a given spot so that the variance caused by moving objects can be filtered as outliers.

9 Conclusions

While the majority of indoor localization systems aim at locating the users themselves based on known floor plans, we aim to locate a signal source in an unknown indoor space. To this end, we have innovatively exploited the power of multipath (which is often “antagonized” by wireless system researchers) and hence proposed a system called iLocScan; it is able to locate a signal source in an indoor space while constructing the floor map of the targeted space at the same time. Leveraging the ability of antenna arrays in detecting the Angle-of-Arrival (AoA) of a signal path, we have implemented iLocScan to the point that it can simultaneously measure all AoAs induced by an indoor wireless transmission (due to its direct path and multiple reflection paths). This has involved fine-tuning a well known AoA detection algorithm and investigating the features of various array patterns. We have also designed a logic module for iLocScan to judge which AoA corresponds to the direct path and whether the number of observed AoAs is a sufficient, as well as an autonomous problem formulation and solving module to fit the variables (source location and space geometry) to the AoAs. To demonstrate the viability of these ideas, we have implemented an iLocScan prototype using USRP2 units. Our extensive experiments with this prototype have strongly confirmed the efficacy of iLocScan and also delivered useful insights on indoor signal reflection and propagation.

10 Acknowledgements

This research is supported in part by AcRF Tier 2 Grant ARC15/11 and Nanyang Centre for Underground Space, NTU. We are grateful to our shepherd Shyam Gollakota and anonymous reviewers for their valuable comments, as well as to Syed Naveen A.A. from Institute for Infocomm Research (I²R), Singapore for the inspiring discussions with him.

11 References

- [1] P. Bahl and V. Padmanabhan. RADAR: an In-building RF-based User Location and Tracking System. In *Proc. of 19th IEEE INFOCOM*, pages 775–784, 2000.
- [2] P. Bolliger. Redpin - Adaptive, Zero-configuration Indoor Localization Through User Collaboration. In *Proc. of the ACM MELT*, pages 55–60, 2008.
- [3] K. Chintalapudi, A. Padmanabha Iyer, and V. N. Padmanabhan. Indoor Localization Without the Pain. In *Proc. of the 16th ACM MobiCom*, pages 173–184, 2010.
- [4] T. Coleman and Y. Li. An Interior, Trust Region Approach for Nonlinear Minimization Subject to Bounds. *SIAM Journal on Optimization*, 6:418445, 1996.
- [5] Y. Jiang, X. Pan, K. Li, Q. Lv, R. P. Dick, M. Hannigan, and L. Shang. ARIEL: Automatic Wi-Fi Based Room Fingerprinting for Indoor Localization. In *Proc. of the 14th ACM UbiComp*, pages 441–450, 2012.
- [6] X. Jie and J. Kyle. ArrayTrack: A Fine-grained Indoor Location System. In *Proc. of the 10th USENIX NSDI*, pages 71–84, 2013.
- [7] P. Lazik and A. Rowe. Indoor Pseudo-ranging of Mobile Devices using Ultrasonic Chirps. In *Proc. of the 10th ACM SenSys*, pages 99–112, 2012.
- [8] F. Li, C. Zhao, G. Ding, J. Gong, C. Liu, and F. Zhao. A Reliable and Accurate Indoor Localization Method Using Phone inertial Sensors. In *Proc. of the 14th ACM UbiComp*, pages 421–430, 2012.
- [9] H. Lim, C. Kung, J. Hou, and H. Luo. Zero Configuration Robust Indoor Localization: Theory and Experimentation. In *Proc. of the 25th IEEE INFOCOM*, pages 1–12, 2006.
- [10] H. Liu, Y. Gan, J. Yang, S. Sidhom, Y. Wang, Y. Chen, and F. Ye. Push the Limit of WiFi Based Localization for Smartphones. In *Proc. of the 18th ACM MobiCom*, pages 305–316, 2012.
- [11] J. Luo, H. Shukla, and J.-P. Hubaux. Non-Interactive Location Surveying for Sensor Networks with Mobility-Differentiated ToA. In *Proc. of the 25th IEEE INFOCOM*, pages 1241–1252, 2006.
- [12] R. Nandakumar, K. K. Chintalapudi, and V. N. Padmanabhan. Centaur: Locating Devices in an Office Environment. In *Proc. of the 18th ACM Mobicom*, pages 281–292, 2012.
- [13] J.-g. Park, B. Charrow, D. Curtis, J. Battat, E. Minkov, J. Hicks, S. Teller, and J. Ledlie. Growing an Organic Indoor Location System. In *Proc. of the 8th ACM MobiSys*, pages 271–284, 2010.
- [14] A. Rai, K. K. Chintalapudi, V. N. Padmanabhan, and R. Sen. Zee: Zero-effort Crowdsourcing for Indoor Localization. In *Proc. of the 18th ACM MobiCom*, pages 293–304, 2012.
- [15] N. Ravi and L. Iftode. FiatLux: Fingerprinting Rooms using Light Intensity. In *Proc. of the 5th Pervasive*, 2007.
- [16] J. Sallai, A. Lédeczi, and P. Völgyesi. Acoustic Shooter Localization with a Minimal Number of Single-channel Wireless Sensor Nodes. In *Proc. of the 9th ACM SenSys*, pages 96–107, 2011.
- [17] T. Schmidl and D. Cox. Robust Frequency and Timing Synchronization for OFDM. *IEEE Trans. on Communications*, 45(12):1613–1621, 1997.
- [18] R. Schmidt. Multiple Emitter Location and Signal Parameter Estimation. *IEEE Trans. on Antennas and Propagation*, 34(3):276–280, 1986.
- [19] S. Sen, J. Lee, K. Kim, and P. Congdon. Avoiding Multipath to Revive Inbuilding WiFi Localization. In *Proc. of the 11th ACM MobiSys*, pages 249–262, 2013.
- [20] S. Sen, B. Radunovic, R. R. Choudhury, and T. Minka. You Are Facing the Mona Lisa: Spot Localization Using PHY Layer Information. In *Proc. of the 10th ACM MobiSys*, pages 183–196, 2012.
- [21] P. Setlur and N. Devroye. Multipath Exploited Bayesian and Cramér-Rao Bounds for Single-Sensor Target Localization. *EURASIP Journal on Advances in Signal Processing*, 53:1–23, 2013.
- [22] H. Wang, S. Sen, A. Elgohary, M. Farid, M. Youssef, and R. R. Choudhury. No Need to War-drive: Unsupervised Indoor Localization. In *Proc. of the 10th ACM MobiSys*, pages 197–210, 2012.
- [23] K. Whitehouse, C. Karlof, and D. Culler. A Practical Evaluation of Radio Signal Strength for Ranging-based Localization. *ACM/SIGMOBILE Mob. Comput. Commun. Rev.*, 11(1):41–52, 2007.
- [24] O. Woodman and R. Harle. Pedestrian Localisation for Indoor Environments. In *Proc. of the 10th UbiComp*, pages 114–123, 2008.
- [25] J. Xiong and K. Jamieson. SecureAngle: Improving Wireless Security Using Angle-of-arrival Information. In *Proc. of the 9th ACM HotNets*, pages 11:1–11:6, 2010.
- [26] M. Youssef and A. Agrawala. The Horus WLAN Location Determination System. In *Proc. of the 3rd ACM MobiSys*, pages 205–218, 2005.
- [27] M. Youssef, A. Youssef, C. Rieger, U. Shankar, and A. Agrawala. Pin-Point: An Asynchronous Time-Based Location Determination System. In *Proc. of the 4th ACM MobiSys*, pages 165–176, 2006.
- [28] C. Zhang, K. Subbu, J. Luo, and J. Wu. GROPING: Geomagnetism and cROwdsensing Powered Indoor Navigation. *IEEE Trans. on Mobile Computing*, (available online), 2014.